Journal of Membrane Science 556 (2018) 178–184

Contents lists available at ScienceDirect

Journal of Membrane Science

journal homepage: www.elsevier.com/locate/memsci

Interaction between membrane and organic compounds studied by atomic force microscopy with a tip modification

Hui Lei[a,*], Na Cheng[b], Jianwei Zhao[b,*]

[a] GE (China) Research and Development Center, Shanghai 201203, China
[b] College of Material and Textile Engineering, China-Australia Institute for Advanced Materials and Manufacturing, Jiaxing University, Jiaxing 314001, China

ARTICLE INFO

Keywords:
Atomic force microscopy
Reverse osmosis membrane
Organic fouling
Force curve

ABSTRACT

Membrane fouling by organic, inorganic and biological materials is a significant cause of the increased operational costs in the membrane separation processes such as reverse osmosis, nanofiltration, ultrafiltration and microfiltration. To better understand the fouling mechanism and increase the membrane performance via optimizing membrane structure, elucidation of the physicochemical interactions between membranes and foulants is essential. Atomic force microscopy (AFM) has been proved to be a powerful method to qualitatively characterize the interaction force between the tip and the substrate. In this paper, the AFM tips were modified to bear five representative organic end-groups: benzyl, hexyl, propionic acid, ethylamine hydrochloride, sodium propyl sulfonate, which are commonly found in organic foulants. The adhesion force between the modified AFM tip and the reverse osmosis membrane was measured carefully to understand the potential fouling tendency of each category function group on the membrane. The results showed the average interaction force between the tip modified by -$(CH_2)_3$-SO_3Na group and membrane is 13.80 nN, which is as twice as the force between membrane and the unmodified tip. The results also showed that the tips modified by -$(CH_2)_2$-COOH group and -$(CH_2)_3$-SO_3Na group, have stronger interaction force with the membrane surface than the tips modified by three other end-groups, which indicated these two kinds of organic compounds are easier to deposit on the membrane surface and cause membrane fouling. It should be possible to use the method developed in this paper to predict the organic fouling on other types of membranes beyond reverse osmosis membrane.

1. Introduction

Membrane separation processes play a very important role in the separation industry. Microfiltration, ultrafiltration, nanofiltration, reverse osmosis (RO) are widely used membrane separation processes, and their difference is based on separation mechanisms and size of the separated particles. Membrane separation processes are now widely used in waste water treatment, drinking water treatment and ultra-pure water production.

Fouling, i.e., flux reduction with time, is one of the most serious concerns in the application of membrane processes [1–4]. Membrane fouling caused by organic, inorganic and biological materials is a significant cause of increased operational costs and energy consumption for membrane separation processes such as reverse osmosis, nanofiltration, ultrafiltration and microfiltration. This phenomenon depends on many factors, like feed characteristics, membrane apparatus type, membrane characteristics and operational procedures etc. Many approaches have been examined to minimize the impact of membrane fouling, such as improving the membrane module design [5,6], changing membrane surface properties [7–12], optimizing operation conditions [13], developing effective pretreatment [14,15] and cleaning methods [16,17]. The basic mechanism of these approaches is to decrease the interaction between membrane and foulants to reduce the deposition of foulants on the membrane surface. Elucidation of the physicochemical interactions between membranes and foulants is needed for understanding the fouling mechanism and minimize the membrane fouling.

Atomic force microscopy (AFM) [18] has been used to get information about the surface properties with a molecular-scale resolution. AFM is becoming a powerful tool in the field of membrane technology [19–23]. The technique has been applied to provide useful membrane information [24–27] about surface morphology, surface pore size and its distribution, surface porosity and measure force interactions between the sharp tip of a cantilever and specimen surface as a function of probe-surface separation distance [28]. Especially AFM can image surfaces and measure the force interactions in air and in liquid without any special sample treatment. In several research papers [29,30], it has already been demonstrated that the AFM force

* Corresponding authors.
E-mail addresses: leihuilh@hotmail.com (H. Lei), jwzhao@mail.zjxu.edu.cn (J. Zhao).

https://doi.org/10.1016/j.memsci.2018.04.002
Received 7 March 2018; Received in revised form 4 April 2018; Accepted 4 April 2018
Available online 05 April 2018
0376-7388/

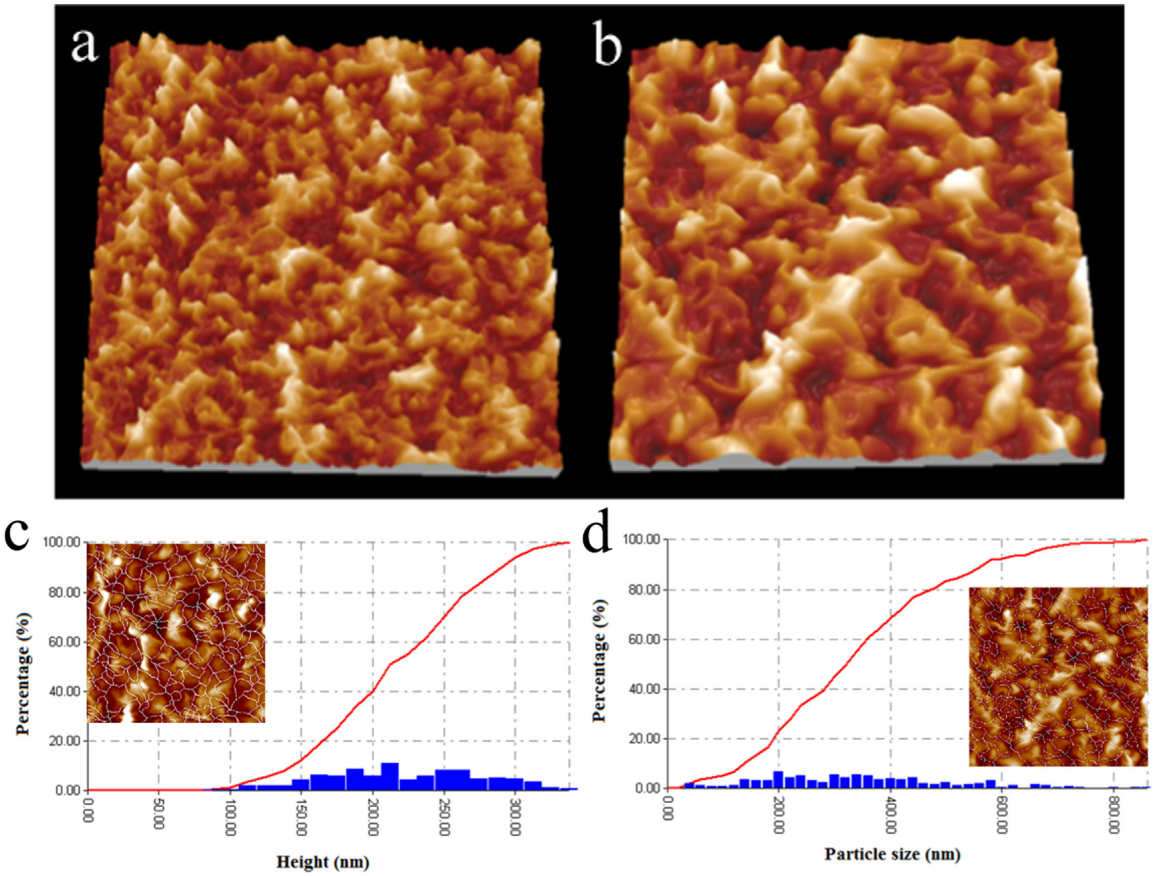

Fig. 1. AFM images and surface particles size and height analysis of RO membrane (a) membrane area 10 µm × 10 µm; (b) membrane area 5 µm × 5 µm; (c) particle height distribution curve; (d) particle size distribution curve.

measurement for quantification of the affinity between a modified colloid particle on the cantilever and the surfaces of nano-filtration/reverse osmosis membranes.

The fundamental mechanism controlling the fouling of RO membranes is complex and not well understood. AFM would be a very useful method to help people understand the mechanism of fouling, such as the interaction between foulants and membrane, then control it. The purposes of this paper is to assess membrane-organics interaction by using the AFM technique. In this study AFM tips modified by different organic groups are used to measure the interaction between organic groups and membrane surface.

2. Experimental

2.1. Materials

The membrane used in this study was brought from GE Water & Process Technologies. AFM Cr-Au tips were from Mikromasch and chemicals 4-Methylbenzenethiol (SH-C_6H_4-CH_3), 1-Hexanethiol (SH-$(CH_2)_5$-CH_3), 3-Mercaptopropionic acid (SH-$(CH_2)_2$-COOH), Cysteamine hydrochloride (SH-$(CH_2)_2$-NH_3Cl), Sodium 3-mercapto-1-propanesulfonate (SH-$(CH_2)_3$-SO_3Na) used for modification of AFM Cr-Au tips were purchased from Sigma-Aldrich.

2.2. Preparation of modified AFM tips

To evaluate the interaction force between the organic foulants and the membrane, a tip modification strategy was adopted in this study [31,32] This method not only allows us to test a series of model foulants, but also provides a reliable force measurement due to the reduced interfacial fraction between the modified tip and substrate [33] Especially, a self-assembly technique [34] has been demonstrated to be useful to obtain a relatively well-ordered monolayer even on the nanosized tip. The modified tips used in the AFM force measurement were prepared by the following procedure [33]. First, the AFM Cr-Au tips were soaked in 100 mL 1.0 mmol/L ethanol solution of the modifying molecule for 24 h. Then, the modified Cr-Au tips were rinsed thoroughly with ethanol and super-pure water respectively to remove the contaminants on the tips. The bare Cr-Au tips were prepared by being soaked in ethanol solvent for 24 h as a control sample.

2.3. AFM image and interfacial force measurement

An atomic force microscope (OpenSYS from Benyuan Nano Equipment Co, Ltd., China) was used to capture the membrane surface image and measure interfacial force. Measurements were done in air with 20–40% humidity and by using contact operation mode. Taken the heterogeneities of membrane surfaces into account, force curves measurement on one membrane were made by four AFM tips and each at 15 different locations. At each location 30 force curves were tested. So total 1800 force curves between each type of modified AFM tips and membrane sample (30 curves/location × 15 locations/tip × 4 tips = 1800 at least) were obtained to represent the interaction between tip and membrane. Gaussian fitting was chosen to analyze the data and the peak position, *Xc*, was obtained to represent the interaction force.

All force curves obtained by the AFM force measurement were expressed as a function of force and separation distance. On AFM force curves, the separation distance at which the interaction became either repulsive or attractive was identified as the point where the measured force was either positive or negative, respectively.

Based on the force curve, the slope of the line (s) could be calculated

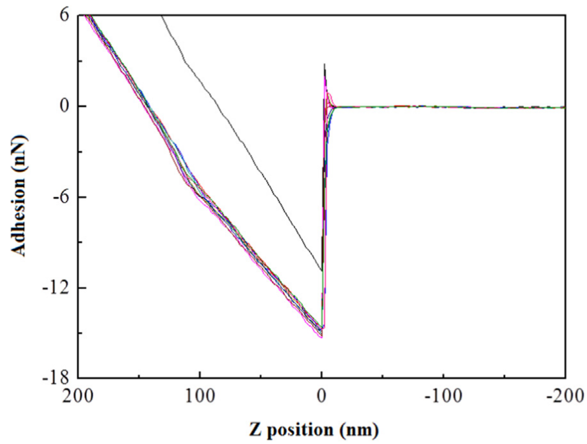

Fig. 2. Example of statistical results summary of 50 force curves between unmodified AFM tips and RO membrane.

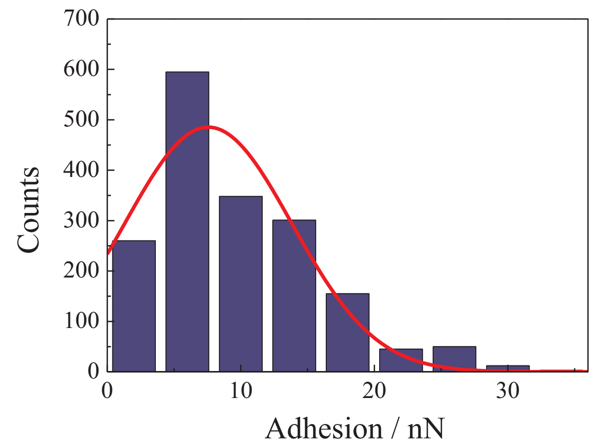

Fig. 3. Statistical summary of 1800 force curves between unmodified AFM tips and RO membrane.

where the separation distance x was negative. The deformation degree Δx could be calculated by the equation $\Delta x = z \times \Delta y/s$, where Δy was the absolute value of the minimum force and z was the strictive coefficient with value of 10.93 nm/V for the used equipment. The adhesion force F could be obtained by the equation $F = \mathrm{k} \times (\Delta x)$, which k was the force constant of the AFM tip with value of 0.12 N/m.

3. Results and discussion

3.1. Surface morphology of RO membrane

The surface morphology is one of the most important membrane properties. Study on the membrane surface morphology can help to understand the cause-and-effect relationships among membrane morphology, membrane fouling and membrane performance. Fig. 1 shows typical 3D AFM images of RO membrane over areas of 10 µm × 10 µm (Fig. 1a) and 5 µm × 5 µm (Fig. 1b). Different color represents the vertical deviations in the sample with the white regions being the highest and the dark regions the lowest. The AFM images obtained are so distinct and that membrane surface structures are clearly captured. The color intensity in the images reflects the vertical profile of the membrane surface with the light regions as the highest points and the dark regions as the lowest points. Both pictures (Fig. 1a and b) show a typical RO membrane surface structure. The whole membrane surface is covered by humps with different height, which is an inherent property of interfacially polymerized aromatic polyamide composite membranes. The humps are uniform over the observed area and the size is about 150–500 nm, which is fully in agreement with the typical RO membrane surface structures reported in other research paper [35].

From the sample morphology, we further analyze the surface roughness with a statistical summary for the samples. Usually, a good mathematical analysis requires large scanned area. However, the resolution of AFM images decreases with the scan area increasing. The image resolution decreases with increase of the surface area. Higher resolution can be achieved when the area is smaller. But for the smaller membrane area, less number of humps is covered. While the scanned area is too large, the decreased resolution may cause relatively large error statistically. On the contrary, a small scan range is not representative for the whole sample. The scan range of several micrometers is reasonable, because this scale includes a few tens of the specific structural features. In order to represent the typical membrane morphology and reasonable statistical analysis, we chose the membrane area of 10 µm × 10 µm and 5 µm × 5 µm.

The statistical analysis results of typical samples are compared in Fig. 1(c) and (d). In the present sample, the average peak-valley height is 215.3 nm, and less than 10% points have height from 0 to 137.nm, and less than 50% have height from 0 to 200 nm, and less than 90% have height from 0 to 287.5 nm. The root-mean-square roughness (RMS) value of this RO membrane is 43.3 nm, which is substantially less than those values of most other types of RO membranes [35]. Different roughness of membrane surface is due to the different membrane formula and manufacture process. The smoother membrane surface is, the lower fouling in operation it causes due to the low tendency of foulants tracked in the valley and easy removal of the foulants on membrane surface.

In Fig. 1(d), the average particle size is 305.63 nm, and the percentage of size from 0 to 140 nm is less than 10%. The percentage of size from 0 to 260 nm is less than 50%, and the percentage of size from0 to 500 nm was less than 90%. The measurements were performed at different locations with membrane area of 10 µm × 10 µm and 5 µm × 5 µm. There is no significant difference between the results of different locations. The membrane surface is covered by uniform layer with average particle size of 305.63 nm which is much larger than the radius of AFM tips (20–30 nm). So interfacial force measurement from AFM tips and membrane surface is believed to be the pure interaction between tip molecular and membrane material.

3.2. The force curve measurement of the unmodified AFM tip

In order to prove the feasibility of the experiment design, originally unmodified tip was used as the control method to measure the interaction force between tip and membrane. Four new Cr-Au tips were immersed in ethanol solvent for over 24 h and washed with ethanol and pure water to remove the contaminants before use. Fig. 2 shows 10 typical force curves of the unmodified AFM tip on the RO membrane at one location. When the AFM tip removed from the membrane surface, the adhesion force between tip and membrane increases with increase of the distance. The adhesion force keeps increased till a critical value. After that, the adhesion force suddenly jumps to zero, which indicates the tip is not touching the sample surface. In general, the repeatability of this measurement is good except very few curves on which the adhesion force was much less or bigger than others. The possible reason for that could be the micro structure, transient contamination, or turbulence from the thermal drift. For example, when the tip stabs into a polymer valley, the adhesion force is much enhanced due to the large contact area. Also vibration of tip could happen when it bounces off the membrane surface.

In order to obtain reliable experiment results, usually a large amount of measurements between tip and one membrane were made and statistical analysis is used to represent the interaction. A statistical average of more than 400 individual adhesive force measurements using Gaussian fit was used to represent the adhesion force between tip

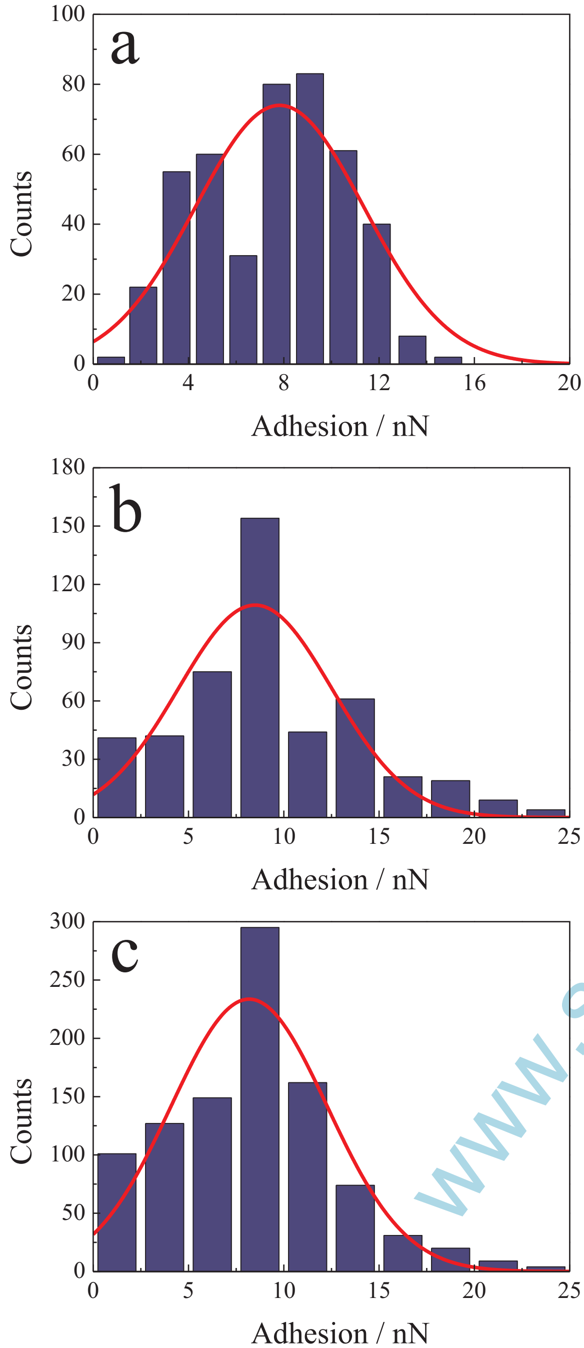

Fig. 4. (a) Statistical summary of first 500 force curves between -$(CH_2)_5$-CH_3 modified AFM tips and RO membrane; (b) Statistical summary of second 500 force curves between -$(CH_2)_5$-CH_3 modified AFM tips and RO membrane; (c) Statistical summary of total 1000 force curves between -$(CH_2)_5$-CH_3 modified AFM tips and RO membrane.

and sample in Zhang's research [36]. Wang [37] also reported a statistical average of 300–500 force-distance curves obtained at different points on the sample as the tip was moved over the surface. In this paper, due to the variation of interaction measurement by AFM, measurements with large number of repeats for one sample were applied to get more accurate results. For each tip, 15 different locations were measured and at each location 30 force curves were tested. So totally 1800 force curves were obtained to explain the interaction force between the various tips and RO membrane. The force curves from different tips were compared and the repeatability was reasonably good, and the repeatability of force curves from one tip but different locations

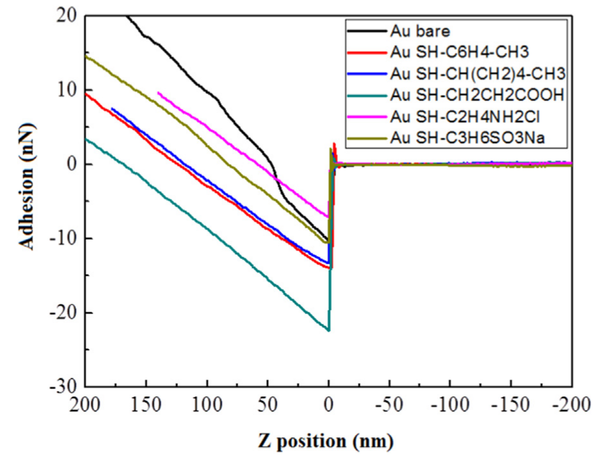

Fig. 5. Force curve between unmodified/modified AFM tips and RO membrane.

was also good enough, which meant the repeatability of this experiment was good and results was reliable. The interaction force between unmodified tip and RO membrane was calculated from the statistical summary of all the tested curves. Gaussian fitting was chosen to analyze the data as also adopted by other researchers [36,38] and peak position, *Xc*, was obtained to express the interaction force showed in Fig. 3. The interaction force between unmodified tip and RO membrane was 7.56 nN with standard error of 1.01 nN.

3.3. Evaluation of the reliability of the adhesive force of the modified tips

Fouling is a big challenge for RO membrane application, and organic fouling is one of the major fouling issues. The typical organic foulants includes alkane, aromatic, acid, anionic and cationic organics. Therefore, in this paper, -C_6H_4-CH_3, -$(CH_2)_5$-CH_3, -$(CH_2)_2$-COOH, -$(CH_2)_2$-NH_3Cl, -$(CH_2)_3$-SO_3Na were chosen as representative organic groups to modify the AFM tips and mimic the organic fouling of RO membrane.

Although the reliability for the unmodified AFM tip was tested as discussed before, it is still unknown whether this method is valid while the tip is covered by a monolayer of organic compound. In the present study, a self-assembly technique was used to form the organic monolayer on the tip. It has been widely demonstrated that the thiol group can be robustly immobilized on the gold surface with a covalent bond after 24 h soaking [34]. However, it is still a big question whether the modified monolayer remains after several tens punches to the membrane substrate. Therefore, we firstly tested the stability of the monolayer during force measurements. The -$(CH_2)_5$-CH_3 monolayer was chosen as an example to demonstrate if the modified groups were moved away from the tip surface after several times testing. Fig. 4 shows the statistical summary of first and second 500 force curves, and total 1000 force curves. Fig. 4a shows the statistical distribution of the counts of the first 500 force curves that gives peak position of 7.83 nN with standard error of 0.56 nN. Fig. 4b gives the statistical result of the second 500 force curves with 8.49 peak position and 0.84 standard error. Fig. 4c summarize all 1000 force curve and gives 8.17 nN peak position and 0.57 nN standard error. This comparison proves the reliability of the test. The summary showed no significant difference between the first, second 500 force curves and total 1000 force curves, indicating that the interaction between organic group and AFM tips was strong and the results obtained from different time were consistent. It is not difficult to be understood, while we recognized that the organic monolayer serves as the lubricant between the tip and the substrate. [39,40].

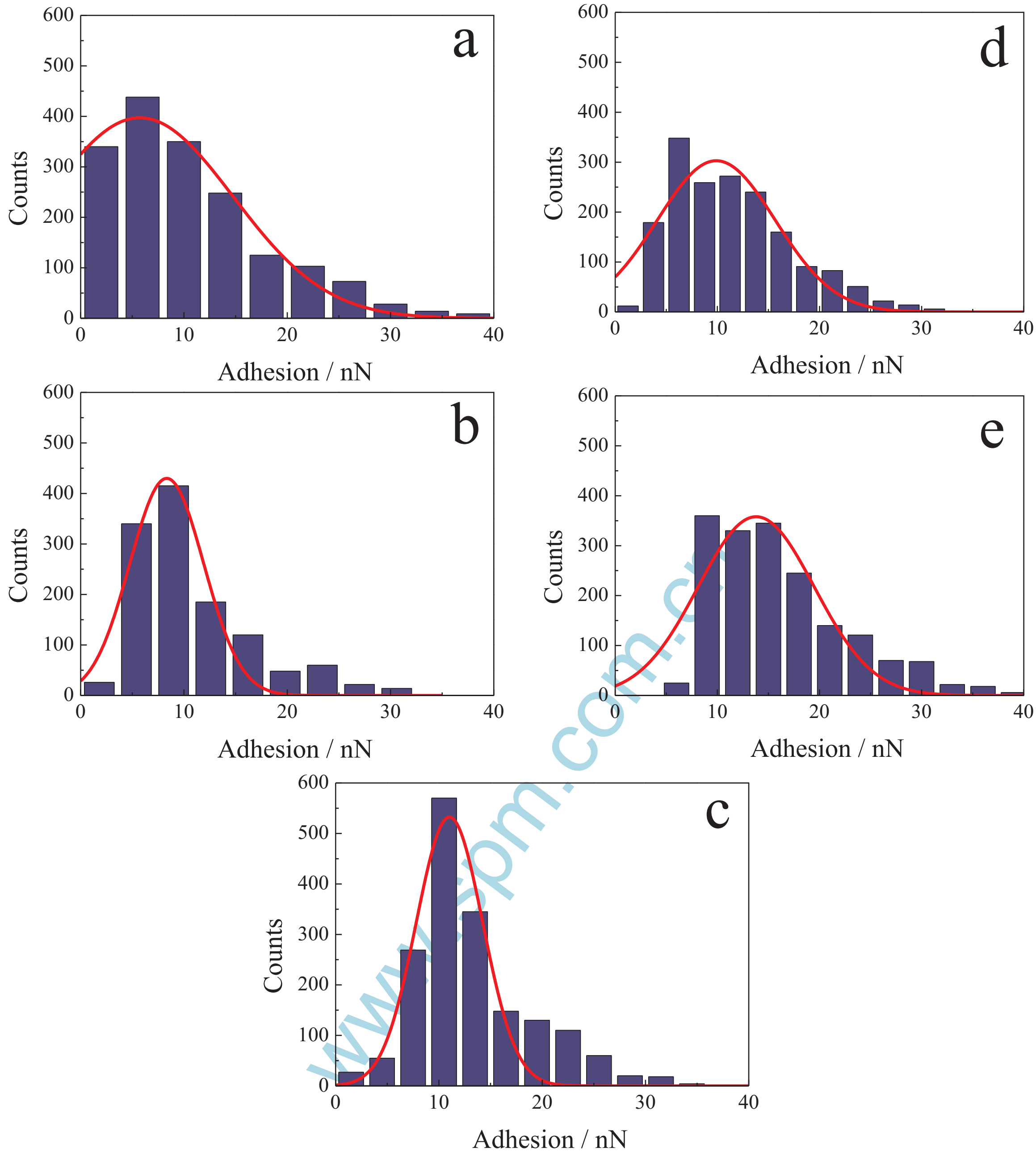

Fig. 6. Statistical summary of adhesion between different organic group modified tip and RO membrane (a) -C_6H_4-CH_3 (b) -$(CH_2)_5$-CH_3 (c) -$(CH_2)_2$-COOH (d) -$(CH_2)_2$-NH_2.HCl (e) -$(CH_2)_3$-SO_3Na.

Table 1
Summary of adhesion force between different organic groups modified tip and RO membrane.

Organic group	Adhesion Force Xc (nN)	Standard error (nN)
Unmodified tip	7.56	1.01
-C_6H_4-CH_3	5.73	0.65
-$(CH_2)_5$-CH_3	8.34	0.45
-$(CH_2)_2$-COOH	11.02	0.37
-$(CH_2)_2$-NH_3Cl	9.89	0.63
-$(CH_2)_3$-SO_3Na	13.80	0.81

3.4. Measurement of the interaction between the modified tips and membrane

The main reason for quantifying the interactions between a modified tip and a membrane by AFM is to quantify the propensity of the surface to foul in use. The interaction force between the modified tips and RO membrane was measured by the same testing procedure as used for the previous unmodified tips and membrane. Fig. 5 shows force curves between unmodified/modified tips and RO membrane, and here just shows one representative curve of each modified tip. The repeatability for the force curves between one modified tip and membrane meets the requirement of the force measurement. After modification, the adhesion force between tips and membrane changed, compared with the force between unmodified tip and membrane, which meant the interaction between different organic group and membrane surface was different.

In order to get more accurate results, four tips were modified with one organic group and used for the force curve measurement. For each modified tip, 15 different locations were measured, at each location 30 force curves were tested and total 1800 force curves were obtained to elaborate the interaction between modified tips and RO membrane. Fig. 6 shows the statistical summary of the interaction between different organic groups modified tips and membrane, and Lorenz fitting was used to analyze the data and Xc was calculated to express the interaction force. The detailed interaction forces between modified tips and RO membrane were summarized in Table 1. The adhesion force of different organic group modified tips and RO membrane was different. The tips modified by -C_6H_4-CH_3 group had the weakest adhesion to membrane surface, possibly due to the fact that phenyl group is similar to the membrane chemistry. The tips modified by -$(CH_2)_2$-COOH group and -$(CH_2)_3$-SO_3Na group had stronger adhesion to membrane surface than other groups, which might be due to the higher ionic strength of these two groups. The stronger interaction means that these organic groups are easier to deposit on membrane surface which causes membrane fouling. This method can be used to predict the organic fouling tendency of RO membrane. The study on membrane fouling using synthetic organic salt water will be done in the future. In order to get the membrane with low fouling tendency, the membrane design with smooth membrane surface and neutral charge is desired to decrease the interaction between foulants and membrane surface so as to decrease the foulants deposition.

4. Conclusion

In this paper a new method was developed to measure the interaction between membrane and organics. The curve about relationship between the adhesion force and the distance of AFM tip and membrane surface was obtained by AFM. The adhesion force between unmodified tip, five modified tips by different organic groups (C_6H_4-CH_3, $(CH_2)_5$-CH_3, $(CH_2)_2$-COOH, $(CH_2)_2$-NH_2HCl, $(CH_2)_3$-SO_3Na) and RO membrane were measured. To get reliable results, 1800 force curves of each tip were tested, and statistical method was used to calculate the adhesion force. The adhesion force between $(CH_2)_3$-SO_3Na modified tip reaches 13.8 nN which is about twice of the hydrophobically modified tips, such as C_6H_4-CH_3 and $(CH_2)_5$-CH_3 and unmodified tips. These results indicate that the hydrophilic organic groups are easier to deposit on membrane surface and cause membrane fouling. This paper provides a convenient way with almost no need to prepare membrane sample, to predict the organic fouling tendency of RO membrane. In the future, it should be possible to use the method developed here to allow pre-assessment on the organic fouling possibility of process water with different types of membranes. This should allow optimum membrane selection with no need for pilot tests and huge cost saving.

Acknowledgements

Many thanks to GE (China) Research and Development Center team members for their generous help on the experiments and sharing of knowledge. Many thanks also to the Professor Zhao's team and graduated students in Nanjing and Jiaxing University for their great help and support on the experiments.

References

[1] Q. She, R. Wang, A.G. Fane, C.Y. Tang, Membrane fouling in osmotically driven membrane processes: a review, J. Membr. Sci. 499 (2016) 201–233.
[2] H. Lin, M. Zhang, F. Wang, F. Meng, B.Q. Liao, H.C. Hong, J.R. Chen, W.J. Gao, A critical review of extracellular polymeric substances (EPSs) in membrane bioreactors: characteristics, roles in membrane fouling and control strategies, J. Membr. Sci. 460 (2014) 110–125.
[3] F. Qu, H. Liang, J. Zhou, J. Nan, S. Shao, J. Zhang, G. Li, Ultrafiltration membrane fouling caused by extracellular organic matter (EOM) from Microcystis aeruginosa: effects of membrane pore size and surface hydrophobicity, J. Membr. Sci. 449 (2014) 58–66.
[4] H. Yamamura, K. Kimura, Y. Watanabe, Mechanism involved in the evolution of physically irreversible fouling in microfiltration and ultrafiltration membranes used for drinking water treatment, Environ. Sci. Technol. 41 (2007) 6789–6794.
[5] J.Y. Kim, I.S. Chang, D.H. Shin, H.H. Park, Membrane fouling control through the change of the depth of a membrane module in a submerged membrane bioreactor for advanced wastewater treatment, Desalination 231 (2008) 35–43.
[6] X. Huang, G.R. Guillen, E.M.V. Hoek, A new high-pressure optical membrane module for direct observation of seawater RO membrane fouling and cleaning, J. Membr. Sci. 364 (2010) 149–156.
[7] H.Y. Yu, Y. Kang, Y. Liu, B. Mi, Grafting polyzwitterions onto polyamide by click chemistry and nucleophilic substitution on nitrogen: a novel approach to enhance membrane fouling resistance, J. Membr. Sci. 449 (2014) 50–57.
[8] G. Kang, M. Liu, B. Lin, Y. Cao, Q. Yuan, A novel method of surface modification on thin-film composite reverse osmosis membrane by grafting poly (ethylene glycol), Polymer 48 (2007) 1165–1170.
[9] H. Karkhanechi, R. Takagi, H. Matsuyama, Biofouling resistance of reverse osmosis membrane modified with polydopamine, Desalination 336 (2014) 87–96.
[10] D.L. Shaffer, H. Jaramillo, S.R.V. Castrillón, X. Lu, Improving the fouling resistance of brackish water membranes via surface modification with graphene oxide functionalized chitosan, Desalination 365 (2015) 99–107.
[11] S. Asim, M. Wasim, A. Sabir, M. Shafig, H. Andlib, S. Khuram, A. Ahmad, T. Jamil, The effect of Nanocrystalline cellulose/Gum Arabic conjugates in crosslinked membrane for antibacterial, chlorine resistance and boron removal performance, J. Hazard. Mater. 343 (2018) 68–77.
[12] M. Wasim, A. Sabir, M. Shafig, A. Islam, M. Azam, T. Jamil, Mixed matrix membranes: two step process modified with electrospun (carboxy methylcellulose sodium salt/sepiolite) fibers for nanofiltration, J. Ind. Eng. Chem. 50 (2017) 172–182.
[13] H.K. Vyas, R.J. Bennett, A.D. Marshall, Influence of operating conditions on membrane fouling in crossflow microfiltration of particulate suspensions, Int. Dairy J. 10 (2000) 477–487.
[14] C. Yang, L. Li, J. Shi, C. Long, A. Li, Advanced treatment of textile dyeing secondary effluent using magnetic anion exchange resin and its effect on organic fouling in subsequent RO membrane, J. Hazard. Mater. 284 (2015) 50–57.
[15] K. Li, H. Liang, F. Qu, S. Shao, H. Yu, Z. Han, X. Du, G. Li, Control of natural organic matter fouling of ultrafiltration membrane by adsorption pretreatment: comparison of mesoporous adsorbent resin and powdered activated carbon, J. Membr. Sci. 471 (2014) 94–102.
[16] X. Li, T. Cai, G.L. Amy, T.S. Chung, Cleaning strategies and membrane flux recovery on anti-fouling membranes for pressure retarded osmosis, J. Membr. Sci. 522 (2017) 116–123.
[17] A. Al-Amoudi, R.W. Lovitt, Fouling strategies and the cleaning system of NF membranes and factors affecting cleaning efficiency, J. Membr. Sci. 303 (2007) 4–28.
[18] G. Binnig, C.F. Quate, C. Gerber, Atomic force microscope, Phys. Rev. Lett. 56 (1986) 930–933.
[19] N. Hilal, W.R. Bowen, L. Alkhatib, O. Ogunbiyi, A review of atomic force microscopy applied to cell interactions with membranes, Chem. Eng. Res. Des. 84 (2006) 282–292.
[20] W.R. Bowen, N. Hilal, R.W. Lovitt, C.J. Wright, Direct measurement of interactions between adsorbed protein layers using an atomic force microscope, J. Colloid Interface Sci. 197 (1998) 348–352.
[21] W.R. Bowen, N. Hilal, R.W. Lovitt, C.J. Wright, A new technique for membrane characterisation: direct measurement of the force of adhesion of a single particle using an atomic force microscope, J. Membr. Sci. 139 (1998) 269–274.
[22] W.R. Bowen, N. Hilal, R.W. Lovitt, C.J. Wright, Direct measurement of the force of adhesion of a single cell using an atomic force microscope, Colloids Surf. A: Physicochem. Eng. Asp. 136 (1998) 231–234.
[23] W.R. Bowen, N. Hilal, R.W. Lovitt, C.J. Wright, Atomic force microscopy as a tool for the membrane technologist, Microsc. Anal. 68 (1998) 13–16.
[24] A. Bessieres, M. Meireles, R. Coratger, J. Beauvillain, V. Sanchez, Investigations of surface properties of polymeric membranes by near field microscopy, J. Membr. Sci. 109 (1996) 271–284.
[25] W.R. Bowen, T.A. Doneva, Atomic force microscopy studies of nanofiltration membranes: surface morphology, pore size distribution and adhesion, Desalination 129 (2000) 163–172.
[26] W.R. Bowen, T.A. Doneva, J.A.G. Stoton, The use of atomic force microscopy to quantify membrane surface electrical properties, Colloids Surf. A: Physicochem. Eng. Asp. 201 (2002) 73–83.
[27] D. Johnson, N. Hilal, Characterisation and quantification of membrane surface properties using atomic force microscopy: a comprehensive review, Desalination 356 (2015) 149–164.
[28] W.R. Bowen, T.A. Doneva, H.B. Yin, Atomic force microscopy studies of membrane—solute interactions (fouling), Desalination 146 (2002) 97–102.
[29] D. Johnson, F. Galiano, S.A. Deowan, J. Hoinkis, A. Figoli, N. Hilal, Adhesion forces between humic acid functionalized colloidal probes and polymer membranes to assess fouling potential, J. Membr. Sci. 484 (2015) 35–46.
[30] W.R. Bowen, N. Hilal, R.W. Lovitt, C.J. Wright, Atomic force microscope studies of membrane surfaces, in: T.S. Sørensen (ed.). Surface Chemistry and Electrochemistry of Membrane Surfaces, Surfactant Science Series, 79, 1999, pp. 1–37.
[31] J. Zhao, J.J. Davis, Force dependent metalloprotein conductance by conducting atomic force microscopy, Nanotechnology 14 (2003) 1023–1028.
[32] D. Axford, J.J. Davis, N. Wang, D. Wang, T. Zhang, J. Zhao, B. Peters, Molecularly resolved protein electromechanical properties, J. Phys. Chem. B 111 (2007) 9062–9068.
[33] J. Zhao, J.J. Davis, M.S.P. Samson, A. Hung, Exploring the electronic and mechanical properties of protein using conducting atomic force microscopy, J. Am. Chem. Soc. 126 (2004) 5601–5609.
[34] A. Ulman, An Introduction to Ultrathin Organic Films, Academic Press, Boston, MA, 1991.
[35] S.-Y. Kwaka, D.W. Ihm, Use of atomic force microscopy and solid-state NMR

spectroscopy to characterize structure-property-performance correlation in high-flux reverse osmosis (RO) membranes, J. Membr. Sci. 158 (1999) 143–153.
[36] H. Zhang, H.X. He, T. Mu, Z.F. Liu, Force titration of amino group-terminated self-assembled monolayers of 4-aminothiophenol on gold using chemical force microscopy, Thin Solid Films 327–329 (1998) 778–780.
[37] B. Wang, R.D. Oleschuk, P.M. Petkovich, J.H. Horton, Chemical force titrations of antigen- and antibody-modified poly(methylmethacrylate), Colloids Surf. B: Biointerfaces 55 (2007) 107–114.
[38] A. Noy, C.D. Frisbie, L.F. Rozsnyai, M.S. Wrighton, C.M. Lieber, Chemical force microscopy: exploiting chemically-modified tips to quantify adhesion, friction, and functional group distributions in molecular assemblies, J. Am. Chem. Soc. 117 (1995) 7943–7951.
[39] Q. Zhang, L.A. Archer, Boundary lubrication and surface mobility of mixed alkylsilane self-assembled monolayers, J. Phys. Chem. B 107 (2003) 13123–13132.
[40] Q. Zhang, L.A. Archer, Interfacial friction of surfaces grafted with one- and two-component self-assembled monolayers, Langmuir 21 (2005) 5405–5413.